Received: 25 March 2024 | Revised: 5 July 2024 | Accepted: 12 July 2024

DOI: 10.1111/jfb.15885

REGULAR ARTICLE

JOURNAL OF FISH BIOLOGY fsbi

Parauchenoglanis stiassnyae (Siluriformes: Auchenoglanididae): A new species of giraffe catfish from Mfimi-Lukenie basin, central Africa, Democratic Republic of Congo

Myriam Y. Modimo[1] | Maxwell J. Bernt[2] | Raoul J. C. Monsembula Iyaba[1] | José J. M. M. Mbimbi[1] | Tobit L. D. Liyandja[1,3,4]

[1]Department of Biology, University of Kinshasa, Kinshasa, Democratic Republic of the Congo

[2]Department of Biology, Susquehanna University, Selinsgrove, Pennsylvania, USA

[3]Department of Biological Sciences, University of Toronto Scarborough, Toronto, Canada

[4]Department of Natural History, Royal Ontario Museum, Toronto, Canada

Correspondence
Tobit L. D. Liyandja, Department of Biological Sciences, University of Toronto Scarborough, Toronto, Canada.
Email: tobit.liyandja@utoronto.ca; tobit.liyandja@rom.on.ca and tobit.liyandja@unikin.ac.cd

Funding information
National Science Foundation Graduate Research Fellowship Program, Grant/Award Number: 1655227; Axelrod Research curatorship (MJLS)

Abstract

A new, distinctively short-bodied giraffe catfish of *Parauchenoglanis* is described from the Ndzaa River, a small left-bank tributary of the Mfimi-Lukenie basin in the Central basin of the Congo River in the Democratic Republic of the Congo. The new species can be distinguished from all congeners by having 29 or fewer (vs. 33 or more) total vertebrae. It can further be distinguished from all congeners, except *Parauchenoglanis zebratus* Sithole et al., 2023 and *Parauchenoglanis ngamensis* (Boulenger 1911), by having 13 or 14 (vs. 16 or more) pre-anal vertebrae. The species is endemic to the Mfimi River basin, where it has been collected mainly in blackwater tributaries.

KEYWORDS
Congo basin, CT scan, DNA barcoding, morphology, Ndzaa River, *Parauchenoglanis*

1 | INTRODUCTION

With only three genera currently recognized and 21 valid species (Fricke et al., 2024), the African catfish family Auchenoglanididae, recently separated from the family Claroteidae (Lundberg et al., 2007), is one of the less diverse African catfish families. For example, its most closely related family, Claroteidae (Lundberg et al., 2007; Schedel et al., 2022), has three times more species (Fricke et al., 2024). However, this lack of recorded diversity likely reflects taxonomic confusion, poorly defined species and genera (Geerinckx et al., 2013), and the existence of species complexes (Sithole et al., 2023). Among the three auchenoglanidid genera currently recognized (Geerinckx et al., 2013), *Parauchenoglanis* Boulenger, 1911 is the most diverse, with 10 recognized species (Ferraris 2007, Sithole et al., 2023, Fricke et al., 2024).

Parauchenoglanis was erected by Boulenger (1911) to accommodate two *Auchenoglanis* species, *Auchenoglanis guttatus* and *Auchenoglanis macrostoma*, that he noted were significantly different from *Auchenoglanis* sensu stricto (Geerinckx et al., 2004). Jordan (1920) designated *Pimelodus guttatus* (Lönnberg 1895) as the type species of *Parauchenoglanis*, yet only after the work of Teugels et al. (1991) was *Parauchenoglanis* clearly defined and delineated (Geerinckx et al., 2004). The taxonomic history of *Parauchenoglanis* encompasses 18 nominal species described across the African continent. A systematic revision of the genus conducted by Geerinckx et al. (2004) reduced the number of valid *Parauchenoglanis* species to nine. However, species delimitation and diagnostic characters for *Parauchenoglanis* species still remain poorly defined.

In a recent study describing a new species, *Parauchenoglanis zebratus*, Sithole et al. (2023) highlighted cryptic diversity of

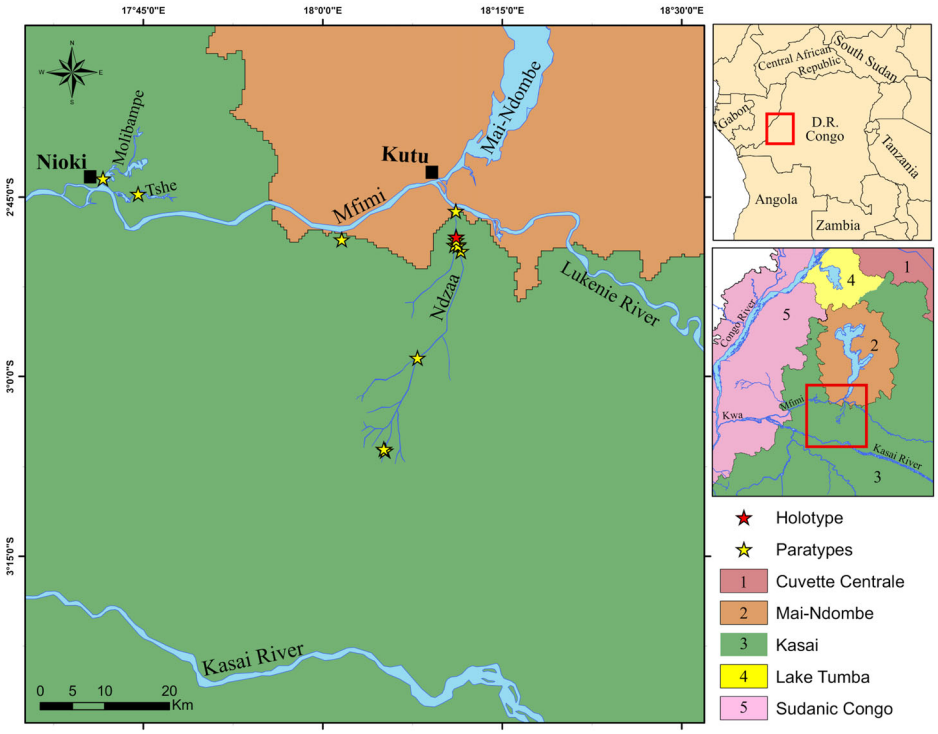

FIGURE 1 Map indicating the location of the Ndzaa River and distribution of *Parauchenoglanis stiassnyae* sp. nov. in the Mfimi-Lukenie basin. Colored areas represent different ecoregions following Abell et al. (2008).

Parauchenoglanis in central and southern Africa, detecting several undescribed lineages. However, the latter study did not include specimens from the central Congo basin. In a recent study of fishes of the Mfimi River in the central Congo basin of the Democratic Republic of the Congo (DRC), two species of Auchenoglanididae were reported (Stiassny, Alter, Liyandja, et al., 2021): *Parauchenoglanis punctatus* (Boulenger 1902) and *Notoglanidium macrostoma* (Pellegrin 1990). One of the three specimens of "*N. macrostoma*," including in the type series herein described, was collected in the Ndzaa River (Figure 1), a small left-bank tributary of the Mfimi River, itself a tributary of the Kasai drainage in the DRC. Stiassny, Alter, Liyandja, et al.'s (2021) assignments of these specimens to *N. macrostoma* were based on examination of external morphology of a few juvenile specimens. Subsequent expeditions to the Ndzaa River, between August and October 2021, June and July 2022, and August and September 2023, allowed the collection of several additional specimens of varying sizes. A more in-depth morphological and osteological study of these specimens coupled with molecular analyses indicated that they represent an undescribed lineage of *Parauchenoglanis*. The objective of this study is to provide a formal description of this new species of giraffe catfish from the Ndzaa River.

The Ndzaa is a left-bank tributary entering the Mfimi, at ~290 m a.s.l., near the settlement of Kutu (Mai-Ndombe Province, DRC) at the outflow of Lake Mai-Ndombe, upstream of which the river is named the Lukenie. The Ndzaa (also known as Ndjua or Ndjuw River) is a tea-colored stream meandering through dense riparian forest surrounded by open grasslands and savannah. The Ndzaa originates in southern Kutu territory, near the city of Semendwa, at ~395 m a.s.l., and its catchment drains an area of ~370 km^2 dominated by shrub savannahs and humid forests. The area drained by the Ndzaa River is under a humid tropical climate characterized by two main seasons: a longer wet season (from September to mid-May) and a shorter dry season (from mid-May to late August). The longer wet season is interrupted by a very short dry period from mid-January to mid-February (Bolanzowu et al., 2019). The pH in the Ndzaa River is generally acidic (pH 4.1–5.3) and differs from the characteristically humic and brown-black waters of the central basin of the Congo. The water conductivity is low (10–50 µS/cm), and the river is low in dissolved solids (TDS: 10–70 mg/L).

2 | MATERIALS AND METHODS

2.1 | Ethics statement

Type specimens were collected and euthanized in accordance with guidelines for the use of fishes in research (Jenkins et al., 2014) and ethical considerations for field research (Bennett et al., 2016). The collection and exportation of these fishes were conducted with permission of the Congolese Ministère de l'Agriculture, Secrètariat General à l'Agriculture, Pêche et Elevage, Direction des Pêches (permits 037/DP/SG/AGRIPEL/2016, 03/DP/SG/PEL/2018, and 23/DP/SG/PEL/2021, all on file at American Museum of Natural History [AMNH]).

2.2 | Molecular data collection and analyses

We used the Qiagen Gentra Puregene Tissue Kit and manufacturer's protocols to extract total genomic DNA from four individuals of three *Parauchenoglanis* species from the Ndzaa River: *P. punctatus*, *P.* cf. *punctatus*_L3 (referred to as *Parauchenoglanis monkei* [Keilback

TABLE 1 GenBank and Barcode of Life Data System (BOLD) accession numbers, tissue codes, and catalog numbers for *COI* sequences of *Parauchenoglanis* specimens utilized in this study.

Taxon	Catalog number	Tissue code	*COI*	Publication
Parauchenoglanis balayi	–	A5-36-96	MK074561	Sonet et al., 2018
Parauchenoglanis cf. *pantherinus*	–	A7-31-739	MK074565	Sonet et al., 2018
P. cf. *pantherinus*	–	A7-31-738	MK074566	Sonet et al., 2018
P. cf. *pantherinus*	–	A7-31-602	MK074567	Sonet et al., 2018
Parauchenoglanis cf. *punctatus*	AMNH 278142	AMCC 284824	PP461583	This study
P. cf. *punctatus*	–	A7-31-764	MK074562	Sonet et al., 2018
P. cf. *punctatus*	–	A7-31-754	MK074563	Sonet et al., 2018
P. cf. *punctatus*	–	A7-31-765	MK074564	Sonet et al., 2018
P. cf. *punctatus*	–	A9-29-3533	KT192843	Decru et al., 2016
P. cf. *punctatus*	–	A9-29-3577	KT192848	Decru et al., 2016
P. cf. *punctatus*	AMNH 250764	AMCC 256659	HM418200	Unpublished
P. cf. *punctatus*	AMNH 250860	AMCC 256672	HM418201	Unpublished
P. cf. *punctatus*	–	A9-29-3232	KT192787	Decru et al., 2016
P. cf. *punctatus*	–	A9-29-3240	KT192789	Decru et al., 2016
Parauchenoglanis monkei	–	T391	HG803488	Peart et al., 2014
P. monkei	–	T568	HG803492	Peart et al., 2014
P. punctatus	–	B4-16-1805-J	KX186050	Unpublished
P. punctatus	–	B4-16-1813-J	KX186045	Unpublished
P. punctatus	AMNH 278134	AMCC 284822	PP461584	This study
Parauchenoglanis stiassnyae sp. nov.	AMNH 278138	AMCC 284847	PP461585	This study
P. stiassnyae sp. nov.	AMNH 278139	AMCC 284823	PP461586	This study
Parauchenoglanis sp.	–	B9-17-4663	KT193142	Decru et al., 2016
Parauchenoglanis sp.	–	SAIAB ES08 B148	SAFW418-08	Unpublished
Parauchenoglanis sp.	–	SAIAB ES07 F 041	SAFW237-08	Unpublished
Parauchenoglanis sp.	–	SAIAB ES08 B 308	SAFW563-09	Unpublished
Parauchenoglanis sp.	–	SAIAB ES08 B310	SAFW565-09	Unpublished

Abbreviation: AMCC, Ambrose Monel Cryo Collection; AMNH, American Museum of Natural History.

1910] by Monsembula Iyaba et al., 2013 and as *P. punctatus*_L3 by Sithole et al., 2023), and the new species herein described. We amplified a 652-bp portion of the cytochrome *c* oxidase subunit 1 (*COI*) which was sequenced on a Sanger sequencing platform following the methods of Lowenstein et al. (2011). All sequences have been deposited in GenBank (Table 1). We obtained 28 additional sequences (22 *Parauchenoglanis*, three *Auchenoglanis* [out-group], and three *Notoglanidium* [out-group]) from the Barcode of Life Data System (http://www.barcodinglife.org) and GenBank (www.ncbi.nlm.nih.gov/genbank). We aligned *COI* sequences, trimming extremities, and calculated the percentage divergence between sampled taxa using Geneious Prime 2024.0 (https://www.geneious.com). We conducted exploratory phylogenetic analyses using maximum likelihood (ML) as implemented in IQ-TREE (Nguyen et al., 2015).

2.3 | Morphological data collection and analyses

Institutional abbreviations follow Sabaj (2022), AMCC stands for the Ambrose Monel Cryo Collection of the AMNH. A total of 55 specimens of *Parauchenoglanis* were examined, including six *Parauchenoglanis balayi* Sauvage 1879, four *Parauchenoglanis guttatus*, four *Parauchenoglanis longiceps* Boulenger 1913, five *Parauchenoglanis pantherinus* Pellegrin 1929, eight *P. punctatus*, 10 *P.* cf. *punctatus*_L3, 14 specimens of *Parauchenoglanis stiassnyae* sp. nov. (see description), and four specimens of *Parauchenoglanis ubangensis* Boulenger 1902. Six meristic counts were taken on each specimen. Fin rays were counted under a stereomicroscope and verified using X-ray images. Vertebrae were counted, excluding the terminal preural centrum and Weberian vertebrae, using both X-ray and micro-computed tomography (μCT) scans (for some specimens) (Figure 2). Forty-five standard morphometric measurements following Geerinckx et al. (2004) were taken on each specimen. These measurements were taken point-to-point using a TRESNA SC30 digital caliper with an accuracy of 0.01 mm. Meristic and morphometric data were analysed separately using principal component analysis (PCA) as implemented in the R package FactoMineR (Lê et al., 2008) and the programme PAST 4.12b (Hammer et al., 2001). Morphometric data were analysed as log-transformed proportions of standard length (SL) to account for body size differences between species, except for fin lengths that were

excluded due to fin damage. Invariant meristic counts (simple and branched dorsal-fin rays) were removed from subsequent analyses.

Four specimens of the new taxon and several comparative specimens of other *Parauchenoglanis* species were scanned using µCT at the AMNH Microscopy and Imaging Facility. Scans were made using a GE Phoenix v|tome|x using a 240-kV Nano Tube (General Electric, Fairfield, CT, USA), with resolution ranging from 10.6 to 24.3 µm. Beam energy was 120 kV and 166 mA. Scans were reconstructed using Phoenix datos|x (General Electric, Wunstorf, Germany) and were rendered and edited using VGStudio Max 3.3.4 (Volume Graphics, Heidelberg, Germany).

3 | RESULTS

3.1 | Barcoding and phylogeny

After trimming, we obtained a final alignment of 641 bp, for 32 specimens, including 179 distinct patterns, 162 parsimony-informative, 20 singletons, and 459 constant sites. Both AIC and Bayesian Information Criterion (BIC) selected the transition model with unequal base frequencies, empirical codon frequencies counted from the data, and discrete gamma with four categories (TIM + F + G4) as the best-fit substitution model for the alignment. The percent divergence calculation estimated that *P. stiassnyae* sp. nov. *COI* sequences diverge by more than 8.8% from all other sampled specimens except one from the Itimbiri River (KT193142), from which *P. stiassnyae* sp. nov. differs by only 2% (Table 2). Phylogenetic analyses retrieved the specimen from the Itimbiri River (KT193142) as the sister to *P. stiassnyae* sp. nov., which together form the sister to *P. balayi* from the Kouilou-Niari River system in the Lower Guinean ichthyofaunal province (Figure 3). Further investigation is needed to establish if the Itimbiri River specimens and *P. stiassnyae* sp. nov. are conspecifics or not. We did not have access to the specimens from Itimbiri and could not morphologically verify their identification.

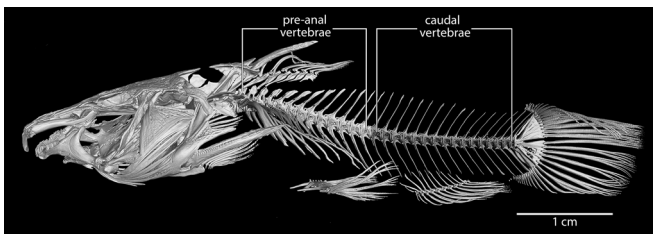

FIGURE 2 Micro-computed tomography (CT) scan the holotype of *Parauchenoglanis stiassnyae* sp. nov. (AMNH 278139), illustrating pre-anal and caudal vertebrae.

3.2 | Meristics

After removal of two invariant counts (unbranched and branched dorsal-fin rays), a PCA was performed on the five remaining meristic counts (caudal-fin rays, anal-fin rays, pre-anal vertebrae, caudal vertebrae, and total vertebrae) for all 55 specimens of the eight examined *Parauchenoglanis* species. We found that 98.5% of variation is explained by the first two principal components, with PC1 accounting for 94.9% and PC2 3.6% of variation. Differences in total, pre-anal, and caudal vertebrae counts contributed most to PC1 factor loadings, with the number of total and pre-anal vertebrae having the highest influence, whereas differences in the number of caudal vertebrae and anal-fin rays contributed most to PC2 loadings. A plot of PC1 against PC2 divided the eight examined *Parauchenoglanis* species into three groups: *P. stiassnyae* sp. nov. was the only member of the first group with the fewest total (28–29) and pre-anal (13–14) vertebrae; the second group, with intermediate total vertebral counts (33–35, mostly 33–34), contains *P. longiceps* and *P. pantherinus*; the third group, with the highest vertebral count (35–38, most with more than 35) includes *P. balayi*, *P. guttatus*, *P. punctatus*, *P.* cf. *punctatus*_L3, and *P. ubangensis* (Figure 4).

3.3 | Morphometrics

A PCA was also performed on 42 morphometric measurements after removal of total length (TL), SL, and pectoral-spine length (due to spine damage) (Figure 5). The first six principal components accounted for 66.2% of total variation with PC1, PC2, and PC3 accounting for 25.1%, 12.7%, and 11.2% of variation, respectively. Differences in the interpectoral distance (5.6%), orbital diameter (4.8%), mouth width

TABLE 2 Distance matrix indicating average percentage difference in partial cytochrome c oxidase subunit I (MT-*COI*) sequences among sampled *Parauchenoglanis*.

Taxon	1	2	3	4	5	6	7	8
1. *Parauchenoglanis balayi*								
2. *Parauchenoglanis* cf. *punctatus* L2	10.6							
3. *P.* cf. *punctatus* L3	8.7	3.7						
4. *Parauchenoglanis* cf. *pantherinus*	9.9	5.2	5.04					
5. *Parauchenoglanis monkei*	10.9	11.3	10.5	10.5				
6. *P. punctatus*	10.4	6.7	5.3	5.6	11			
7. *Parauchenoglanis* sp. KT193142	9.7	10.1	8.5	9.1	11.1	10.4		
8. *Parauchenoglanis* sp. Quanza	10.2	4.7	3.9	5.7	11	5.6	9.2	
9. *Parauchenoglanis stiassnyae*	10.6	9.8	8.9	9.3	11.5	10.5	1.8	9.4

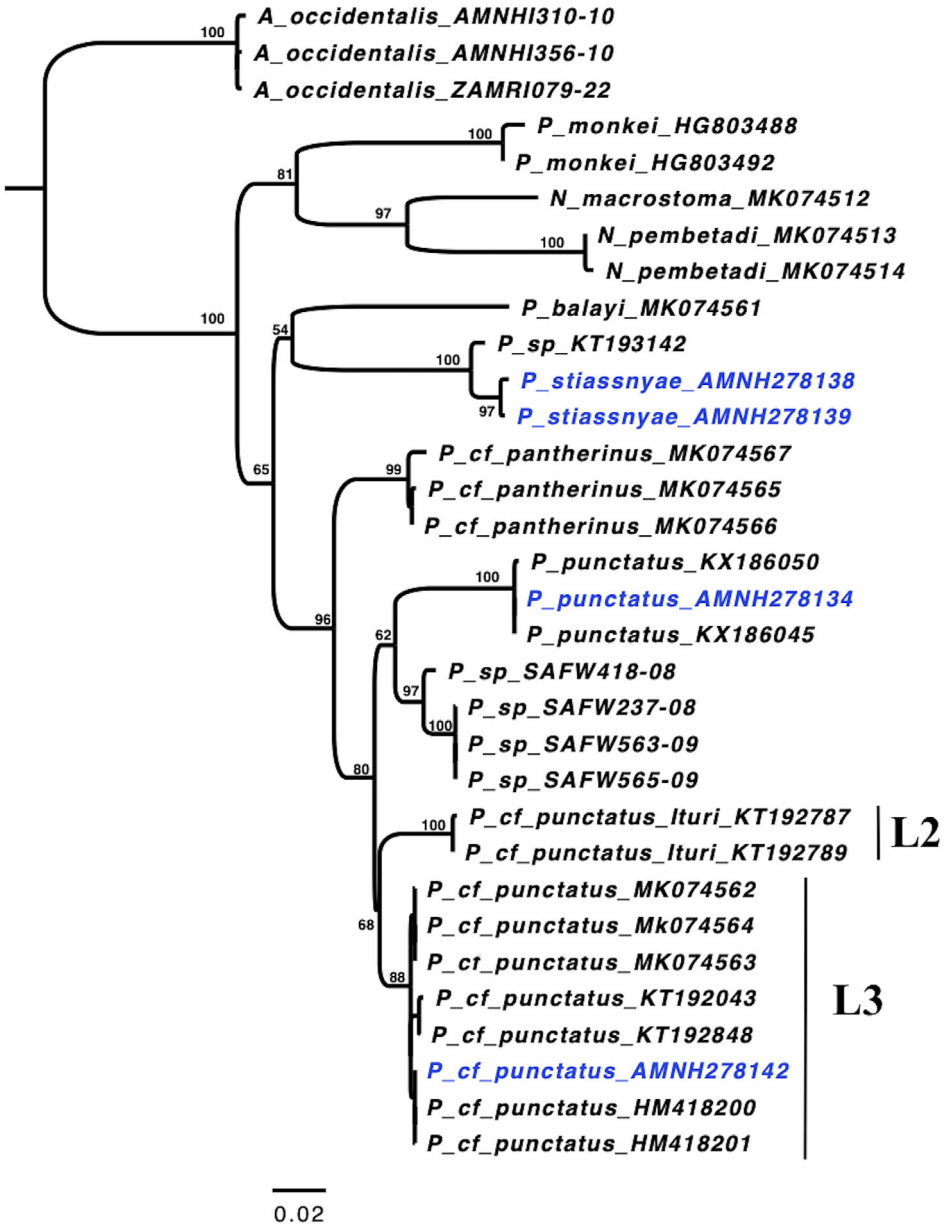

FIGURE 3 Maximum likelihood (ML) hypothesis of possible placement of *Parauchenoglanis stiassnyae* sp. nov. Bootstrap values are reported on/under branches. Sequences generated in this study are indicated in blue. L2 and L3 represent morphologically cryptic lineages of *Parauchenoglanis punctatus* as identified by Sithole et al. (2023).

(4.6%), minimum caudal peduncle height (4.5%), pre-dorsal length (4.1%), and the head width (HW) (4%) contributed the most to PC1 factor loadings, whereas differences in interorbital distance (8.3%), preorbital head length (HL) (8.1%), HL (7.8%), anterior nostrils interdistance (7.6%), supraoccipital process–dorsal-fin interdistance (6.8%), and adipose-fin–caudal-fin interdistance (5.9%) contributed the most to PC2 factor loadings. Differences in pectoral-fin length (7.05%), orbital head height (6.1%), premaxillary toothplate width (5.9%), maximum caudal peduncle height (5.6%), prepectoral length (5.4%), and maximum body height (5.2%) contributed most to PC3 factor loadings. Overall, biplots of PC1 versus PC2 and PC1 versus PC3 divided species into three groups (Figure 5): the first group exclusively contained *P. stiassnyae* sp. nov., the second contained species from Lower Guinea (*P. balayi*, *P. guttatus*, *P. longiceps*, and *P. pantherinus*), whereas the third group contained all remaining species (*P. punctatus*, *P.* cf. *punctatus*_L3, and *P. ubangensis*).

3.4 | Taxonomic description

P. stiassnyae, sp. nov., Zoobank acession numbers: urn:lsid:zoobank.org:act:60B7B236-14C5-497C-9E1A-AAF2DA952047 and urn:lsid:zoobank.org:pub:372F589C-0473-41F7-9873-FA30F1246992.

N. macrostoma: Stiassny, Alter, Liyandja, et al., 2021 and Stiassny, Alter, Monsembula, & Liyandja, 2021.

3.4.1 | Holotype

AMNH 278139 (AMCC 284823), 64.72 mm SL, main channel of the Ndzaa River over mud and plant debris, in forest habitat, ~4.6 km upstream of the Ndzaa confluence with the Mfimi River, Kutu Territory, Mai-Ndombe Province, D. R. Congo, 02°48′17.3″ S, 018°11′08.0″ E, August 10, 2021, M. Y. Modimo.

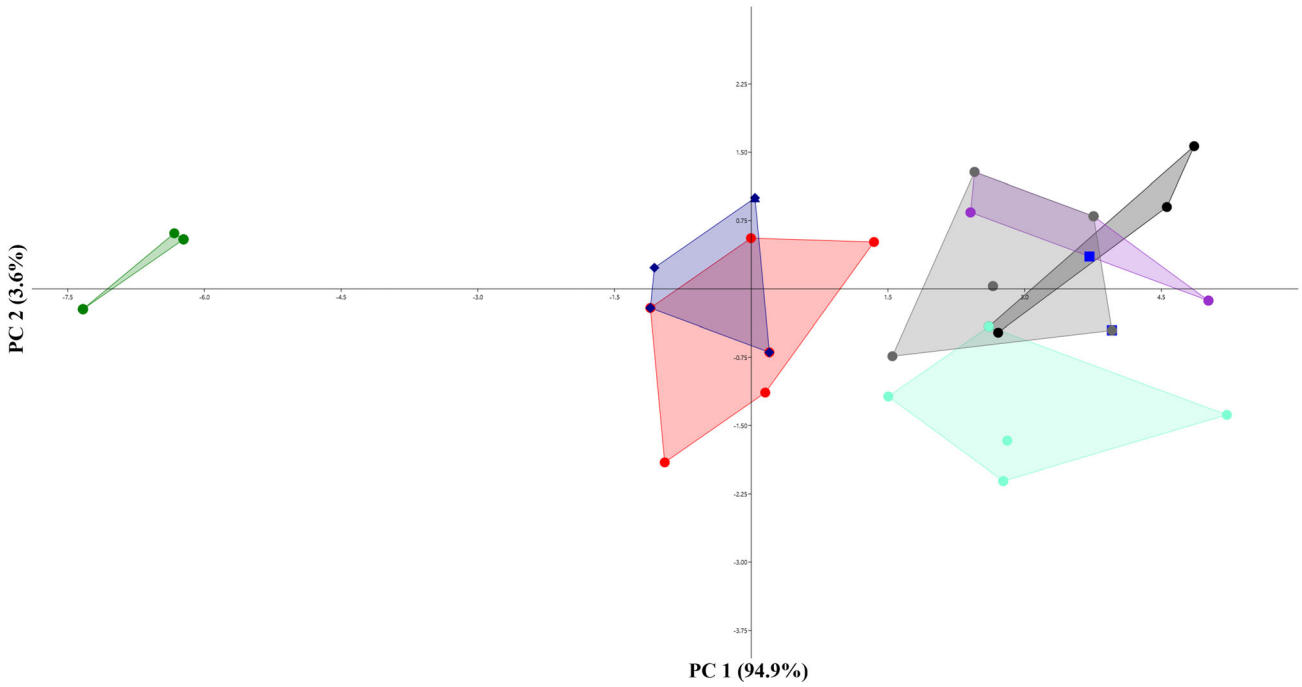

FIGURE 4 Principal component analysis (PCA) biplot of PC1 against PC2 for an analysis of five meristic counts for 55 specimens of sampled *Parauchenoglanis* taxa. *Parauchenoglanis stiassnyae* sp. nov.: ● ; *Parauchenoglanis longiceps*: ◆ ; *Parauchenoglanis pantherinus*: ● ; *Parauchenoglanis guttatus*: ■ ; *Parauchenoglanis ubangensis*: ● ; *Parauchenoglanis* cf. *punctatus*_L3: ● ; *P. punctatus*: ● ; *Parauchenoglanis balayi*: ● .

3.4.2 | Paratypes

$N = 13$. All Mai-Ndombe Province, D. R. Congo: AMNH 278138 (AMCC 284847), 60.22 mm SL, main channel of the Ndzaa River over mud and plant debris, in forest habitat, ~6.9 km upstream of the Ndzaa River confluence with the Mfimi River, Kutu Territory, 02°48′55.8″ S, 018°11′19.0″ E, August 8, 2021, M. Y. Modimo; AMNH 274612 (AMCC 258190), 70.83 mm SL, main channel of the Mfimi River around the Nioki Port, in grass habitat, Kutu Territory, 02°43′25.4″ S, 017°41′38.5″ E, July 20, 2018, Fishermen; AMNH 269908 (two specimens), 66.24–66.28 mm SL, Lebéé River (tributary of Mfimi River) near Kilako village in about 16.7 km downstream of the town of Kutu, over mud, in grass habitat, Kutu Territory, 02°48′30.92″ S, 018°01′34.90″ E, August 8, 2015, R. Monsembula et al.; AMNH 278137 (1, CT-scanned), 73.9 mm SL, main channel of the Ndzaa River over mud and vegetal debris, in forest habitat, in about 7.3 km upstream of the Ndzaa River confluence with the Lukeni River, Kutu Territory, 02°49′29.4″ S, 018°11′31.7″ E, August 7, 2021, M. Y. Modimo; AMNH 278164 (1), 71.7 mm SL, main channel of the Ndzaa River over mud and vegetal debris, in forest habitat, in about 5.5 km upstream of the Ndzaa confluence with the Lukeni River, Kutu Territory, 02°48′35.2″ S, 018°11′09.3″ E, July 25, 2022, R. Monsembula; AMNH 278165 (2), 68.1–70.4 mm SL, in a tributary of Ndzaa River over mud and vegetal debris, in forest habitat, in about 6.3 km upstream of the Ndzaa confluence with the Lukeni River, Kutu Territory, 02°54′58.5″ S, 018°10′59.9″ E, July 24, 2022, R. Monsembula; AUM 86509 (1), 49.8 mm SL, collected with the holotype, M. Y. Modimo, August 10, 2021; MRAC 2024.008.P.0001 (1), 62.55 mm SL, Tshe River (tributary of Mfimi River) in about 5.9 km upstream of Nioki, over mud and vegetal debris, in grass habitat, Kutu Territory, 02°44′42.01″ S, 017°44′33.87″ E, August 2015, R. Monsembula et al.; ROM 112355 (2); 61.8–70.8 mm SL, same location as AMNH 278165, July 30, 2023, R. Monsembula; ZSM 48482 (1), 67.5 mm SL, main channel of the Ndzaa River over mud and vegetal debris, in forest habitat, in about 26.2 km upstream of the Ndzaa River confluence with the Lukeni River, Kutu Territory, 02°58′25.08″ S, 018°07′55.26″ E, July 25, 2018, fishermen.

3.4.3 | Additional non-type material

AMNH 278167 (12); 38.2–57.4 mm SL, collected with ROM 112355; AMNH 278140 (1), 44.3 mm SL, main channel of the Ndzaa River over mud and plant debris, in forest habitat, ~42.2 km upstream of the Ndzaa River confluence with the Lukeni River, Kutu Territory, Mai-Ndombe Province, D. R. Congo, 03°06′10.2″ S, 018°05′14.1″ E, M. Y. Modimo, August 13, 2021; AMNH 278169 (1), 34.1 mm SL, collected with the holotype, August 10, 2021, M. Y. Modimo.

3.4.4 | Diagnosis

P. stiassnyae is distinguished from all congeners by having 28–29 vertebrae (vs. 33 or more). *P. stiassnyae* is also distinguished from all

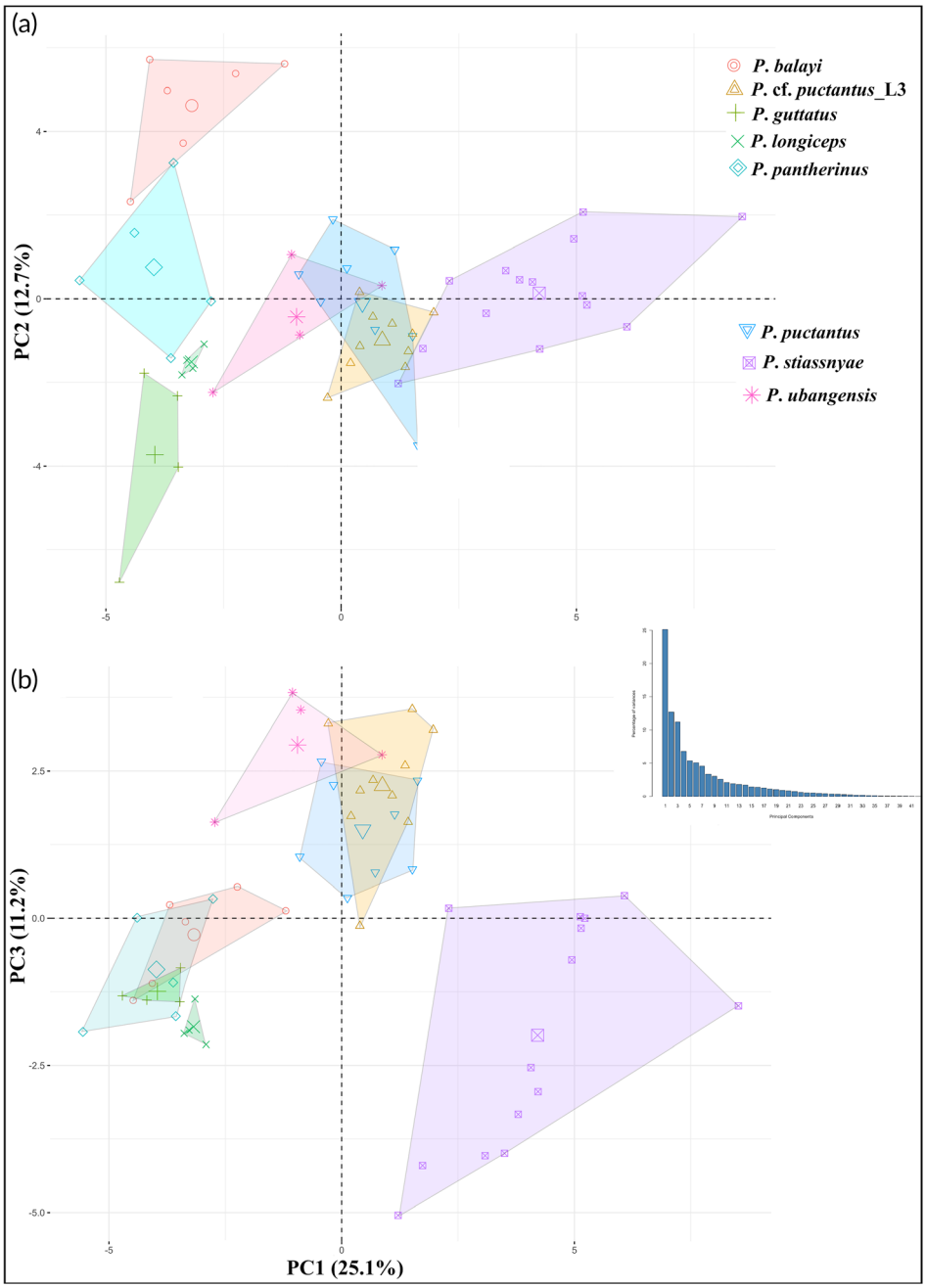

FIGURE 5 Principal component analysis biplots for an analysis of 42 morphometric measurements for 55 specimens of sampled *Parauchenoglanis* taxa: (a) PC1 against PC2 and (b) PC1 against PC3.

congeners by the possession of 13–14 pre-anal vertebrae (vs. 15 or more) except for *Parauchenoglanis zebratus* (14–17) and *Parauchenoglanis ngamensis* (13, holotype). The new species can further be distinguished from *P.* cf. *punctatus*_L3, *P. balayi*, *P. longiceps*, *P. pantherinus*, *P. punctatus*, and *P. ubangensis* by a narrower supraoccipital process–nuchal plate interdistance (1.4%–2.9% vs. >3% HL); from *P.* cf. *punctatus*_L3, *P. guttatus*, *P. longiceps*, *P. pantherinus*, and *P. punctatus* by a wider orbital HW (64.7%–76.2% vs. 54.9%–63.9% HL); from *P. guttatus*, *P. longiceps*, and *P. ubangensis* by a wider mouth (37.8%–50.8% vs. 25.9%–35.7% HL); from *P. guttatus*, *P. punctatus*, *P. ubangensis*, and *P. zebratus* by a wider premaxillary toothplate (12.9%–18.6% vs. 6.6%–12.5% HL); from *P. guttatus*, *P. longiceps*, *P. pantherinus*, and *P. zebratus* by a wider head (HW: 70.1%–81.1% vs. 58.9%–69.3% HL); from *P. balayi* and *P. pantherinus* by a shorter dorsal-fin spine (10.8%–16% vs. 16.1%–18.8% SL); from *P. guttatus* and *P. pantherinus* by a smaller orbital diameter (9.5%–14.2% vs. 14.4%–16.9% HL) and a wider interpectoral distance (16.7%–21.4% vs. 15.3%–16.6% SL); from *P. balayi*, *P. ngamensis* (holotype), and *P. ubangensis* by a shorter adipose-fin–caudal-fin interdistance (2.7%–5.2% vs. 6.2%–10.5% SL); and from *P. balayi* by a longer head (HL: 31.3%–35% vs. 28.1%–30.6% SL) and a narrower interorbital (IOD: 19.5%–27.1% vs. 27.3%–28% HL).

3.4.5 | Description

Based on the holotype and 13 paratypes. General appearance as in Figures 2, 6, and 7 (complete skeleton, external morphology, skull and

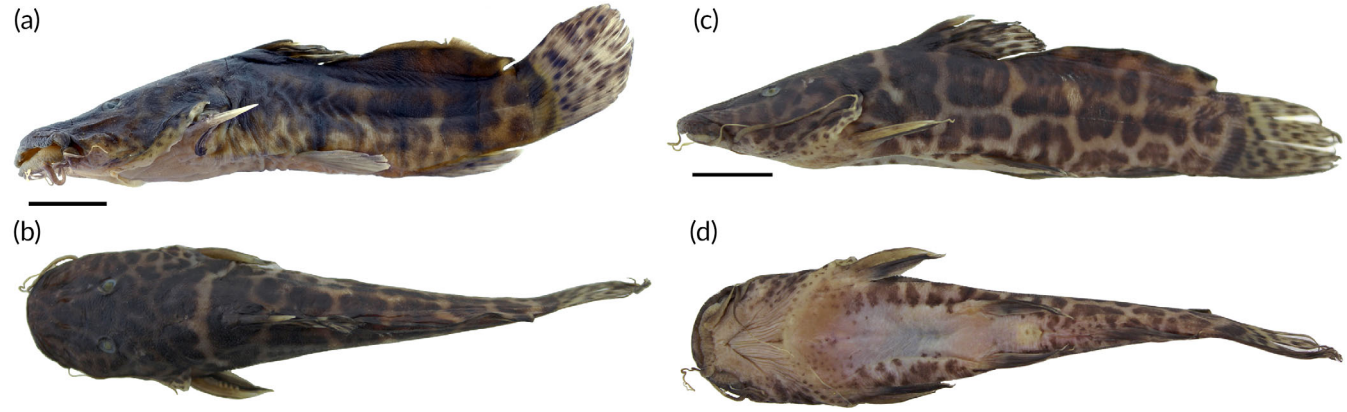

FIGURE 6 Photographs of preserved (a) holotype (AMNH 278139 in lateral view) and (b–d) paratype (AMNH 278165, 68.1 mm standard length [SL], respectively, in dorsal, lateral, and ventral views). Scale bar: 1 cm.

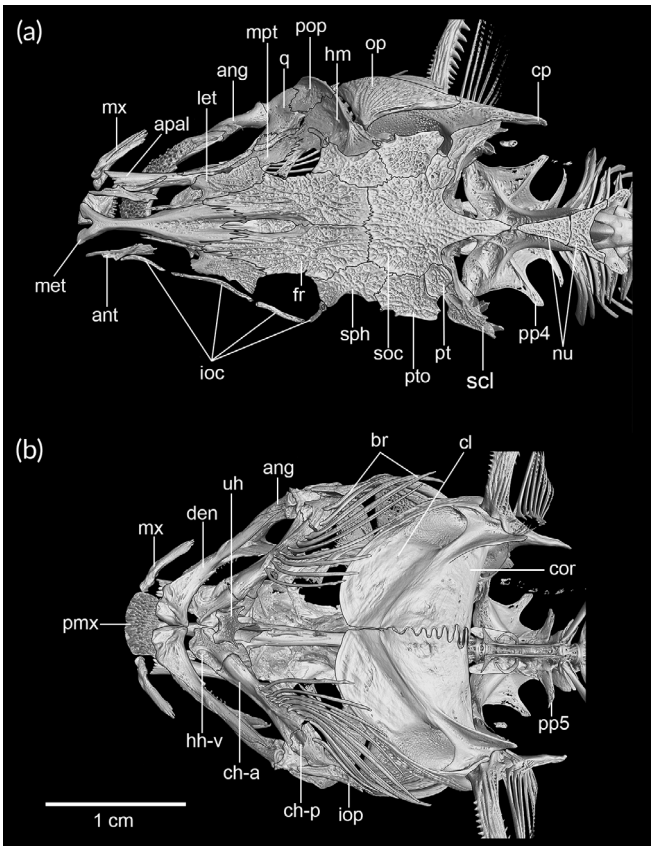

FIGURE 7 Computed tomography scan of the neurocranium of *Parauchenoglanis stiassnyae*, AMNH 269908, paratype, 68.28 mm standard length (SL), in (a) dorsal view with left side of suspensorium removed and (b) ventral view. ang, anguloarticular; apal, autopalatine; br, branchiostegal rays; ch-a, anterior ceratohyal; ch-p, posterior ceratohyal; cl, cleithrum; cp, cleithral process; cor, coracoid; den, dentary; fr, frontal; hh-v, ventral hypohyal; hm, hyomandibula; ioc, infraorbital canals; iop, interopercle; leth, lateral ethmoid; meth, mesethmoid; mpt, metapterygoid; mx, maxilla; nas, nasal; nu, nuchal plates; op, opercle; pmx, premaxilla; pop, preopercle; pp4, parapophysis of 4th vertebra; pp5, parapophysis of 5th vertebra; pop, preopercle; pt, pterotic; pto, posttemporal; q, quadrate; scl, supracleithrum; soc, supraoccipital; sph, sphenotic; uh, urohyal.

pectoral girdle, respectively), proportional measurements in Table 3, and meristic counts in Table 4. Small-bodied species (see Figure 6), maximum observed size 73.9 mm SL (88.3 mm TL; paratype: AMNH 278137), elongate (SL 4.4–6.4 times maximum body height [MxBH]), somewhat dorsoventrally depressed (MxBH 82.4%–109.5% interpectoral distance [IPcD]). Head depressed (head height [HH] 43.5%–58.7% HL, orbital head height [OHH] 28.9%–43% HL, and OHH 38.5%–66.1% orbital head width [OHW]) with very depressed snout (snout height [SnH] 18.1%–26.9% HL) and large terminal mouth (37.8%–50.8% HL). Upper jaw prominent with moderately wide premaxillary toothplate (its width 12.9%–18.6% of the HL) comprising two tooth patches. Branchiostegal rays eight or nine. Maxillary and internal mandibular barbels shorter than HL (their length 51.2%–97.8% HL and 37.2%–77.6% HL, respectively), not surpassing opercular opening. External mandibular barbel generally longer than head (their length 95.4%–147% HL), surpassing tip of adpressed pectoral-fin spine in several specimens. Eye small but not reduced (orbit diameter 9.5%–14.2% HL) and dorsally positioned. Pectoral fin short (length 15.9%–23.1% SL), with seven or eight soft rays, inserted underneath head. Pectoral-fin spine also short (its length 12.9%–18.2% SL) with serrations on both sides. Pelvic fin short with six (one unbranched, five branched) soft rays and generally inserted just posterior to body midline (pre-anal length [PAnL]: 60.3%–72.6% SL). Dorsal fin short (its length 13.3%–18% SL) with two hard and seven soft rays. Dorsal-fin spine also short (10.8%–16% SL), slightly serrated anteriorly, lacking posterior serrations. Caudal fin rounded with 15 or 16 principal rays, including two unbranched. Dorsal surface of neurocranium ornamented with tubercles and with single oblong anterior fontanel. Nuchal plates similarly ornamented on dorsal surface, forming a narrow, anteriorly pointed triangle that surrounds anterior base of dorsal-fin spine (Figure 7a). Anterior bifurcation of mesethmoid narrow, not exceeding posterior mesethmoid width. Infraorbital series present as four narrow cylindrical ossifications. Orbit bordered dorsally by frontal, anteriorly by lateral ethmoid, posteriorly by sphenotic, and ventrally by third and fourth infraorbitals (see Figure 7a). Urohyal trifurcate posteriorly (see Figure 7b). Cleithrum with concave anterior margin and prominent

TABLE 3 Morphometric data for the holotype and 13 paratypes of *Parauchenoglanis stiassnyae*.

Variables	Holotype	Holotype + paratypes		
		Minimum	Maximum	Mean ± SD
Total length (mm)	78.53	62.25	91.14	80.9 ± 7.6
Standard length (mm)	64.72	49.83	73.87	66.1 ± 6.2
Head length (mm)	22.57	16.89	25.14	22.14 ± 2.3
In percentage of standard length (SL)				
Pre-anal length (PAnL)	65.6	60.3	72.6	64 ± 3
Pre-pelvic length (PPvL)	54.9	50.7	56.4	53.8 ± 1.8
Pre-dorsal length (PDL)	42.7	38.7	43.1	41.2 ± 1.2
Prepectoral length (PPcL)	30.8	25.5	33.5	30.2 ± 1.8
Adipose-fin length (AdFL)	31.4	30	42.1	35.7 ± 3.4
Interdorsal–adipose distance (IDAdD)	5.6	1.8	9.8	5.1 ± 2.4
Dorsal-fin base length (DFBL)	17	13.7	20	16.6 ± 1.9
Dorsal-fin length (DFL)	15.2	13.3	18	15.7 ± 1.4
Dorsal-fin spine length (DSL)	14.5	10.8	16	14 ± 1.5
Pectoral-fin length (PcFL)	18.4	15.9	23.1	19.3 ± 1.9
Pectoral-fin spine length (PcSL)	18.1	12.9	18.2	16.3 ± 1.6
Pelvic-fin length (PvFL)	17.9	15.7	21.1	17.6 ± 1.5
Anal-fin length (AFL)	14.1	12.3	18.1	15 ± 1.6
Interpectoral distance (IPcD)	20	16.7	21.4	19.4 ± 1.4
Interpelvic distance (IPvD)	7.5	5.9	7.8	7 ± 0.6
Maximum body height (MxBH)	21.2	15.7	22.7	19.4 ± 2
Pelvic body height (PvBH)	18.2	14.5	20.7	17.4 ± 2
Minimum caudal peduncle height (MnCPH)	15	12.4	15.7	14.3 ± 0.9
Maximum caudal peduncle height (MxCPH)	15.6	13.2	17.4	14.9 ± 1.1
Adipose-fin–caudal-fin interdistance (AdCID)	4	2.7	5.1	4 ± 0.8
Anal-fin–caudal-fin interdistance (AnCID)	14.2	13	16.6	14.5 ± 1.1
Adipose-fin height (AdFH)	7.5	4.7	9.6	6.6 ± 1.3
Head length (HL)	34.9	31.3	35	33.5 ± 1.3
In percentage of head length (HL)				
Postorbital head length (POL)	41.6	41.3	59.2	45.5 ± 4.3
Preorbital head length (PrOL)	52.1	47.8	52.1	49.9 ± 1.6
Head width (HW)	74.1	70.1	81.1	74.9 ± 3.4
Orbital head width (OHW)	70	64.7	76.2	69.6 ± 3.6
Head height (HH)	55.5	43.5	58.7	54.3 ± 4.4
Orbital head height (OHH)	40.5	29	43.2	38.4 ± 3.6
Snout height (SnH)	26.8	18.1	26.9	23.1 ± 2.3
Maxillary barbel length (MxBL)	68.9	51.2	97.8	69.4 ± 12.4
External mandibular barbel length (EMdBL)	107.5	95.4	147	115.8 ± 14.9
Internal mandibular barbel length (IMdBL)	46.5	37.2	77.6	56.3 ± 10.7
Mandibular barbels interdistance (MdBID)	12.3	8.4	17.4	13.5 ± 2.6
Interorbital distance (IOD)	24.1	19.5	27.1	23.3 ± 2.2
Anterior nostrils interdistance (ANID)	24	15.7	24.6	20.7 ± 3
Posterior nostril interdistance (PNID)	12.9	10.1	14.5	12.3 ± 1.4
Supraoccipital process–nuchal plate interdistance (SPNPID)	2.2	1.4	2.9	2.1 ± 0.4
Supraoccipital process–dorsal-fin interdistance (SPDFID)	21	14.9	21	17.4 ± 1.8
Prehyoid length (PHL)	20.3	18.7	23.4	21.2 ± 1.3

(Continues)

TABLE 3 (Continued)

Variables	Holotype	Holotype + paratypes		
		Minimum	Maximum	Mean ± SD
Mouth width (MW)	47.5	37.8	50.8	43.8 ± 4.1
Premaxillary toothplate width (PmxTW)	15.3	12.9	18.6	15.5 ± 1.6
Orbital diameter (OD)	12.9	9.5	14.2	11.9 ± 1.4

Note: Abbreviations follow Geerinckx et al. (2004).

TABLE 4 Meristic data for the holotype and 13 paratypes of *Parauchenoglanis stiassnyae*.

Variables	Holotype	Holotype + paratypes		
		Minimum	Maximum	Mode
Unbranched dorsal-fin rays	2	2	2	2
Branched dorsal-fin rays	7	7	7	7
Anal-fin rays	11	11	12	11
Principal caudal-fin rays	16	15	16	16
Pre-anal vertebrae	13	13	14	13
Caudal vertebrae	16	16	17	16
Total vertebrae	29	29	30	29

humeral processes. Supraoccipital process narrow and sharply pointed.

3.4.6 | Colouration

In preservation, ventral side of the head and body whitish brown to brownish, sometimes with small spots, dorsal side of head and body darker brown. Flanks, head, dorsal fin, and adipose fin with darker brown large spots and light brown vermiculated lines forming a reticulate patterning reminiscent of the distinctive color pattern of the giraffe. Three to four vertical black-dotted bars are visible in some preserved specimens. Dorsal and caudal fins brownish with smaller dark spots. Pectoral, pelvic, and anal fins vary from dark brown to light gray or brown without notable spots. Distal tip of spines (pectoral and dorsal) varies from whitish to light brown, whereas the remaining part (proximal tip) varies from brown to light brown. No live specimens have been examined; however, postmortem pictures taken in the field suggest similar colouration in live specimens.

3.4.7 | Distribution

Currently known only from tributaries of the Mfimi-Lukenie River basin. The holotype, several paratypes, and additional non-type specimens have been collected in the Ndzaa River basin (Figure 1) where the species is widespread. Additional paratypes were collected in the Lobee River (a left-bank tributary of the Mfimi), the Molibampe River at Nioki (right-bank tributary of the Mfimi), and the Tshe River (another right-bank tributary of the Mfimi) upstream of the town of Nioki (Figure 1). However, it should be noted that *P. stiassnyae* only differs by 2% in *COI* sequences from specimens collected in the Itimbiri River 730 km northeast of the Mfimi. Additional collecting throughout the Mfimi River system and the Cuvette Central ecoregion, coupled with further molecular and morphological investigation, will likely extend this species range.

3.4.8 | Biology and ecology

Most specimens of *P. stiassnyae* were collected in forested habitats over mud and plant debris in tributaries of the Mfimi River. The rivers where specimens of *P. stiassnyae* have been collected are characterized by a humic, moderately acidic (pH 4.1–5.3), and dark-brown water with low conductivity (10–50 μS/cm) and low concentrations of dissolved solids (TDS: 10–30 mg/L). These observations, combined with the species body colouration, suggest that *P. stiassnyae* is adapted to forested habitats, muddy, humic, and dark-brown waters of the Mfimi River tributaries.

3.4.9 | Etymology

P. stiassnyae is named after Melanie L. J. Stiassny (MLJS) of the AMHN. MLJS is the initiator of the AMNH Congo Project that resulted in significant documentation and an improved systematic, biological, and evolutionary understanding of the Congo River basin ichthyofauna with an extensive collection deposited at the AMNH, the University of Kinshasa, and the University of Marien Ngouabi. Additionally, MLJS trained and continues to train numerous Congolese ichthyologists, including the authors of the present paper. We dedicate this species to her outstanding work and commitment to biodiscovery and conservation in the Congo River basin.

3.4.10 | Material examined

P. balayi Sauvage 1879 (AMNH 267139, 2 specimens, 115.1–149.7 mm SL, Mpoukou River, Kouilou-Niari basin, collected by Walsh et al. in November 2013; AMNH 258978, three specimens, 133.4–150.5 mm SL, Louesse River, Kouilou-Niari basin, collected by Walsh et al. in January 2012; AMNH 232082, one specimen, 124.6 mm SL, Ivindo River, Ogooué basin, collected by Lahm in May 2000), four *P. guttatus* (AMNH 240688, four specimens, 46.7–94.7 mm SL, Ivindo River, Ogooué basin, collected by Lavoué et al. in July 2007), four *P. longiceps* Boulenger 1913 (AMNH 267131, four specimens, 96.3–119.1 mm SL, Louesse River, Kouilou-Niari basin, collected by Walsh et al. in October 2013), five *P. pantherinus* Pellegrin 1929 (AMNH 267133, three specimens, 79.2–141.1 mm SL, 267133, Louesse River, Kouilou-Niari basin, collected by Walsh et al. in October 2013; AMNH 258980, one specimen, 119.9 SL, Mandoro River, Ogooué basin, collected by Walsh et al. in January 2012; AMNH 256546, one specimen, 70.3 mm SL, Kessampo River, Ogooué basin, collected by Mamonekene in December 2011), eight *P. punctatus* (AMNH 244272, two specimens, 153.1–182.1 mm SL, Sangha River, Congo basin, collected by Mamonekene in September 2006; AMNH 227563, two specimens, 113.7–115.7 mm SL, Sangha River, Congo basin, collected by Sullivan et al. in June 1998; AMNH 274626, two specimens, 88.3–130.2 mm SL, Mfimi River, Congo basin, collected by Stiassny et al. in July 2018; AMNH 278134, one specimen, 128.7 mm SL, Ndzaa River, Congo basin, collected by Modimo et al. in August 2021; AMNH 278135, one specimen, 65.2 mm SL, Ndzaa River, Congo basin, collected by Modimo et al. in August 2021), 10 *P.* cf. *punctatus*_L3 (AMNH 259229, 2 specimens, 73.9–75.3 mm SL, Mayi Ndombe River, Congo basin, collected by Liyandja et al. in July 2011; AMNH 259275, two specimens, 92.3–95.9 mm SL, Mayi Ndombe River, Congo basin, collected by Liyandja et al. in July 2011; AMNH 268756, one specimen, 71.4 mm SL, Kwango River, Congo basin, collected by Liyandja et al. in January 2016; AMNH 259379, one specimen, 71.4 mm SL, Mayi Ndombe River, Congo basin, collected by Liyandja et al. in September 2011; AMNH 259346, four specimens, 72.8–92.3 mm SL, Mayi Ndombe River, Congo basin, collected by Liyandja et al. in September 2011), and four specimens of *P. ubangensis* Boulenger 1902 (AMNH 228563, four specimens, 70.7–103.2 mm SL, Ubangi River, Congo basin, collected by Haroun & Albert in July 1998). All from Gabon: *N. macrostoma*: AMNH 211412 (1, CT-scanned), 180.8 mm SL, Woleu River, Woleu-ogooue, collected by Adriaens et al. in September 2000; AMNH 271727 (1), 154.01 mm SL, Bitoku River, Ngounie, 01°13′57″ S, 010°35′02.3″ E, collected by Cutler & Mve Beh in April 2017; AMNH 262942 (1), 115.3 mm SL, Ogooue-Ivindo, 00°29′01.4″ N, 12°53′33.6″ E, collected by Cutler et al. in April 2014; AMNH 240697 (1), 85.6 mm SL, Bale Creek, Ogooue-Ivindo, 00°31′08.9″ N, 12°47′58.1″ E, collected by Lavoue et al. in July 2007.

4 | DISCUSSION

Sithole et al. (2023) highlighted cryptic diversity in the genus *Parauchenoglanis* in central (Congo basin) and southern Africa. Principally based on their molecular results, they reported the existence of six lineages or candidate species of *Parauchenoglanis* within the boundaries of the Congo basin and suggested that most (66.6%) of these represent cases of species complexes. They also stated that, based on color patterning, *P. zebratus* was the most distinctive of all Congo basin *Parauchenoglanis*. However, our comparison of their morphological dataset for *Parauchenoglanis* species with morphological characteristics of *P. stiassnyae* suggests that *P. stiassnyae* is the most distinctive, both in external morphology (color pattern, body length, and mouth size and shape) and internal anatomy (vertebrae count). In this case, *P. stiassnyae* is not an example of cryptic diversity or part of a species complex but rather a clearly distinct species that has long remained undetected by the scientific community. This highlights how little is known about fishes of the central Congo basin and strengthens the argument for further field and laboratory research to complete species identification guides and checklists needed to monitor and conserve freshwater biodiversity in this region.

Our description of this new *Parauchenoglanis* species is part of an ongoing effort to document and characterize the ichthyofauna of the Mfimi River in the central Congo basin. In a recent study, Stiassny, Alter, Liyandja, et al. (2021) reported that, despite being currently connected to the Kasai basin, the Mfimi fish communities share more affinities with those of the Cuvette Centrale (CC) rather than the fish communities in the rest of the Kasai system (excluding the Kwa). Their conclusion was further supported by the discovery of two new *Phenacogrammus* species endemic to the Mfimi River system (Stiassny, Alter, Monsembula, & Liyandja, 2021). The discovery of *P. stiassnyae* and potentially other endemic new species from this river system reenforce the conclusion that the Mfimi system should be excluded from the Kasai ecoregion. Indeed, in numerous surveys (Mbimbi et al., 2021; Mbimbi & Stiassny, 2011), species descriptions (Liyandja & Stiassny, 2023; Mbimbi & Stiassny, 2012; Van Der Zee et al., 2013; Van der Zee et al., 2015), and collections (in the Kwango, Liyandja unpublished data) conducted in the rest of the Kasai, none has documented the presence of *P. stiassnyae*, *Phenacogrammus flexus* Stiassny, Alter, Liyandja, et al., 2021, or *Phenacogrammus concolor* Stiassny, Alter, Monsembula, & Liyandja, 2021. Absence of these endemic Mfimi species in the rest of the Kasai basin, coupled with the high similarity of the Mfimi fish community with the CC ecoregion, confers a special status to this system.

The initial confusion of *P. stiassnyae* with *N. macrostoma* (Stiassny, Alter, Liyandja, et al., 2021 & Stiassny, Alter, Monsembula, & Liyandja, 2021) was certainly due to external morphological similarity between the two species (including a larger mouth) and the colouration pattern of *P. stiassnyae*, which resembles certain species of the genus *Notoglanidium*. Additionally, the dorsal position of eyes in *P. stiassnyae* is one of the characteristic features used to identify *Notoglanidium* species (Geerinckx et al., 2013). It should be noted that Geerinckx et al. (2013) synonymized several genera with *Notoglanidium* based on morphological data and therefore the boundaries and composition of this genus may change with genetic analyses. Nevertheless, *P. stiassnyae* can be distinguished from all *Notoglanidium* species (sensu Geerinckx et al., 2013) in having a free orbital margin

(vs. subdermal eyes), orbits well demarcated by the frontals and infraorbitals, and a short distance between the supraoccipital and nuchal plate. Further, *P. stiassnyae* is genetically different from *N. macrostoma* (about 12% dissimilarity in *COI* sequences) and can be morphologically distinguished from *N. macrostoma* by its low vertebral count (29–30 vs. 33), smaller mouth (37.8–50.8% vs. 54–63.3% HL) and premaxillary toothplate width (12.9–18.6% vs. 34.3–39.8% HL).

AUTHOR CONTRIBUTIONS

Myriam Y. Modimo and Raoul J.C. Monsembula Iyaba collected the specimens of the new species and environmental data. Maxwell J. Bernt discovered the new species. Tobit L.D. Liyandja, Myriam Y. Modimo, José J. M.M. Mbimbi, and Raoul J.C. Monsembula Iyaba collected the morphometric data. Maxwell J. Bernt collected and analysed µCT-scan data. Tobit L.D. Liyandja and Myriam Y. Modimo extracted DNA, performed PCR, and sequenced the COI. Maxwell J. Bernt and Tobit L.D. Liyandja work on the conceptualization of the study. Tobit L.D. Liyandja performed the analyses. Myriam Y. Modimo, Tobit L.D. Liyandja, José J. M.M. Mbimbi, and Raoul J.C. Monsembula Iyaba wrote the manuscript. All authors read and reviewed the manuscript.

ACKNOWLEDGMENTS

We thank the fishing communities of Kutu and surrounding villages for their help with this project. For logistical support and the issuance of collection and exportation permits, we are grateful to the Ministère de l'Agriculture et du Développement Rural, Sécretariat Général de l'Agriculture, Pêche et Elevage, Direction des Pêches and the Université de Kinshasa, Cabinet du Recteur, the Democratic Republic of the Congo. Our thanks to the collection staff at the AMNH (Radford Arrindell, Tom Vigliotta, and Chloe Lewis) for help in accessioning and cataloging materials from the Ndzaa River collections. We are grateful to Nathan K. Lujan (Royal Ontario Museum) for thoughtful input to the earlier version of the manuscript.

FUNDING INFORMATION

Financial support for the study was provided by the US National Science Foundation (DEB 1655227) and the AMNH Axelrod Research curatorship (MJLS).

CONFLICT OF INTEREST STATEMENT

We declare no conflict of interest.

ORCID

Tobit L. D. Liyandja https://orcid.org/0000-0002-7610-7037

REFERENCES

Abell, R., Thieme, M. L., Revenga, C., Bryer, M., Kottelat, M., Bogutskaya, N., Coad, B., Mandrak, N., Balderas, S. C., Bussing, W., Stiassny, M. L. J., Skelton, P., Allen, G. R., Unmack, P., Naseka, A., Ng, R., Sindorf, N., Robertson, J., Armijo, E., … Petry, P. (2008). Freshwater ecoregions of the world: A new map of biogeographic units for freshwater biodiversity conservation. *Bioscience*, *58*, 403–414.

Bennett, R. H., Ellender, B. R., Makinen, T., Miya, T., Pattrick, P., Wasserman, R. J., Woodford, D. J., & Weyl, O. L. F. (2016). Ethical considerations for field research on fishes. *Koedoe*, *58*, 1–15.

Bolanzowu, M. D., Omasombo, T. J., Stroobant, E., Batamba, A., Krawczyk, J., Laghmouch, M., & Mumbanza, B. J. (2019). *Mai-Ndombe: Mosaique de peuples établie sur un patrimoine naturel*. Tervuren, Belgium: Africamuseum.

Boulenger, G. A. (1911). *Catalogue of the fresh-water fishes of Africa in the British museum (natural history)* (Vol. 2, pp. 1–1529). British Museum (Natural History).

Decru, E., Mooelants, T., De Gelas, K., Vreven, E., Verheyen, E., & Snoeks, J. (2016). Taxonomic challenges in freshwater fishes: A mismatch between morphology and DNA barcoding in fish of the northeastern part of The Congo basin. *Molecular Ecology Resources*, *16*, 342–352.

Ferraris, C. J. (2007). Checklist of catfishes, recent and fossil (Osteichthyes:Siluriformes), and catalogue of siluriform primary types. *Zootaxa*, *1418*, 1–628.

Fricke R., Eschmeyer, W. N., & Van der Laan, R. (2024). *Eschmeyer's catalog of fishes: Genera, species, references*. California Academy of Sciences. Available at: http://researcharchive.calacademy.org/research/ichthyology/catalog/fishcatmain.asp

Geerinckx, T., Adriaens, D., Teugels, G. G., & Verraes, W. (2004). A systematic revision of the African catfish genus *Parauchenoglanis* (Siluriformes : Claroteidae). *Journal of Natura*, *38*, 775–803.

Geerinckx, T., Vreven, E., Dierick, M., Van Hoorebeke, L., & Adriaens, D. (2013). Revision of *Notoglanidium* and related genera (Siluriformes: Claroteidae) based on morphology and osteology. *Zootaxa*, *3691*, 165–191.

Hammer, O., Harper, O., & Rayan, P. (2001). PAST: Paleontological statistics software package for education and data analysis. *Palaeontologia Electronica*, *4*, 1–9.

Jenkins, J. A., Bart, H. L., Bowker, J. D., Bowser, P. R., MacMillan, J. R., Nickum, J. G., Rachlin, J. W., Rose, J. D., Sorensen, P. W., Warkentine, B. E., & Whitledge, G. W. (2014). Guidelines for use of fishes in research, revised and expanded, 2014. *Fisheries*, *39*, 414–416.

Jordan, D. S. (1920). *The genera of fishes, part IV, from 1881 to 1920, thirty-nine years, with the accepted type of each. A contribution to the stability of scientific nomenclature*. Stanford University Press.

Lê, S., Josse, J., & Husson, F. (2008). FactoMineR: An R package for multivariate analysis. *Journal of Statitical Software*, *25*, 1–18. https://doi.org/10.18637/jss.v025.i01

Liyandja, T. L. D., & Stiassny, M. L. J. (2023). Description of two new Labeo (Labeoninae; Cyprinidae) endemic to the Lulua River in the Democratic Republic of Congo (Kasai ecoregion); a hotspot of fish diversity in The Congo basin. *Novitates*, *2023*(3999), 1–24.

Lowenstein, J. H., Osmundson, T. W., Becker, S., Hanner, R., & Stiassny, M. L. J. (2011). Incorporating DNA barcodes into a multi-year inventory of the fishes of the hyperdiverse lower Congo river, with a multi-gene performance assessment of the genus *Labeo* as case study. *Mitochondrial DNA*, *22*, 52–70.

Lundberg, J. G., Sullivan, J. P., Rodiles-Hernandez, R., & Hendrickson, D. A. (2007). Discovery of African roots for the Mesoamerican Chiapas catfish, *Lacantunia enigmatica*, requires an ancient intercontinental passage. *Proceedings of the Academy of Natural Sciences of Philadelphia*, *156*, 39–53.

Mbimbi, J. J. M. M., & Stiassny, M. L. J. (2011). Fishes of the Kwilu River (Kasai basin, central Africa): A list of species collected in the vicinity of Kikwit, Bandundu Province, Democratic Republic of Congo. *Check List*, *7*, 691–699.

Mbimbi, J. J. M. M., & Stiassny, M. L. J. (2012). A new *Alestopetersius* (Characiformes: Alestidae) from the Kwilu River (Kasai basin) of central Africa; with a phylogeny for the genus and synonymy of *Duboisialestes*. *Zootaxa*, *3166*, 59–68.

Mbimbi, J. J. M. M., Stiassny, M. L. J., Monsembula Iyaba, R. J. C., & Liyandja, T. L. D. (2021). Fishes of the lower lulua river (Kasai basin, central africa): A continental hotspot of ichthyofaunal diversity under threat. *Diversity*, *13*(8), 341. https://doi.org/10.3390/d13080341

Monsembula Iyaba, R. J. C., Liyandja, T., & Stiassny, M. L. J. (2013). Fishes of the N'sele river (Pool Malebo, Congo basin, Central Africa): A list of species collected in the main channel and affluent tributaries, Kinshasa Province, Democratic Republic of Congo. *Check List*, *9*, 941–956.

Nguyen, L.-T., Schmidt, H. A., Von Haeseler, A., & Minh, B. Q. (2015). IQ-TREE: A fast and effective stochastic algorithm for estimating maximum-likelihood phylogenies. *Molecular Biology and Evolution*, *32*, 268–274.

Peart, C. R., Bills, R., Wilkinson, M., & Day, J. J. (2014). Nocturnal claroteine catfishes reveal dual colonisation but a single radiation in Lake Tanganyika. *Molecular Phylogenetics and Evolution*, *73*, 119–128.

Sabaj, M. H. (2022). *Codes for natural history collections in ichthyology and herpetology (online supplement)*. Version 9.0 (14 February 2022). American Society of Ichthyologists and Herpetologists. Available from https://asih.org

Schedel, F. D. B., Chakona, A., Sidlauskas, B. L., Popoola, M. O., Usimesa Wingi, N., Neumann, D., Vreven, E. J. W. M. N., & Schliewen, U. K. (2022). New phylogenetic insights into the African catfish families Mochokidae and Austroglanidae. *Journal of Fish Biology*, *100*, 1171–1186.

Sithole, Y., Chakona, A., Musschoot, T., Huyghe, C. E. T., & Vreven, E. J. W. M. N. (2023). A new species of *Parauchenoglanis* (Auchenoglanididae : Siluriformes) from the Upper Lualaba River (Upper Congo), with further evidence of hidden species diversity within the genus. *Journal of Fish Biology*, *102*, 1387–1414.

Sonet, G., Snoeks, J., Nagy, Z. T., Vreven, E., Boden, G., Breman, F. C., Decru, E., Hanssens, M., Ibala Zamba, A., Jordaens, K., Mamonekene, V., Musschoot, T., Van Houdt, J., Van Steenberge, M., Wamuini, L. S., & Verheyen, E. (2018). DNA barcoding fishes from The Congo and the lower Guinean provinces: Assembling a reference library for poorly inventoried fauna. *Molecular Ecology Resources*, *19*, 723–743.

Stiassny, M. L. J., Alter, S. E., Liyandja, T. L. D., Modimo, M. Y., & Monsembula Iyaba, R. J. C. (2021). Fishes of the Mfimi River in the central Congo basin of the Democratic Republic of Congo. Kasai ecoregion or part of the Cuvette Centrale? *Check List*, *17*, 1681–1714.

Stiassny, M. L. J., Alter, S. E., Monsembula, R. J. C., & Liyandja, T. L. D. (2021). Two new *Phenacogrammus* (Characoidei; Alestidae) from the Ndzaa River (Mfimi-Lukenie basin) of central Africa, Democratic Republic of Congo. *American Museum Novitates*, *2021*(3980), 1–22.

Teugels, G. G., Risch, L., De Vos, L., & Thys van den Audenaerde, D. F. E. (1991). Generic review of the African bagrid catfish genera *Auchenoglanis* and *Parauchenoglanis* with description of a new genus. *Journal of Natural History*, *25*, 499–517.

Van Der Zee, J., Mbimbi, J., & Sonnenberg, R. (2013). *Epiplatys atratus* (Cyprinodontiformes: Nothobranchiidae), a new species of the *E. multifasciatus* species group from the Lulua Basin (Kasaï drainage), Democratic Republic of Congo. *Zootaxa*, *3700*, 411–422.

Van der Zee, J. R., Sonnenberg, R., & Mbimbi, J. J. M. M. (2015). *Hypsopanchax stiassnyae*, a new poeciliid fish from the Lulua River (Democratic Republic of Congo) (Teleostei: Cyprinodontiformes). *Ichthyological Exploration of Freshwaters*, *26*, 87–96.

How to cite this article: Modimo, M. Y., Bernt, M. J., Monsembula Iyaba, R. J. C., Mbimbi, J. J. M. M., & Liyandja, T. L. D. (2024). *Parauchenoglanis stiassnyae* (Siluriformes: Auchenoglanididae): A new species of giraffe catfish from Mfimi-Lukenie basin, central Africa, Democratic Republic of Congo. *Journal of Fish Biology*, 1–13. https://doi.org/10.1111/jfb.15885